Supplementary Material

In our calculations, the possible secondary phases include I_2(C*mca* Ibberson et al., 1992), CsI(rock-salt phase), CuI(P*3-m1* Keen and Hull, 1995), AgI(F*4-3m* Adipranoto et al., 2009), AuI(P*42/ncmz* Jagodzinski, 1959), CuI_2(P*1* Dell'amico et al., 1982), AgI_2(P*1* Dell'amico et al., 1982), AuI_2(P*1* Dell'amico et al., 1982), AuI_3(P*121/c1* Clark et al., 1958), Cu_2I_3(P*6*), Ag_2I_3(P*6*), $CsCuI_2$(P*4/nmmz* Hull and Berastegui, 2004), $CsAgI_2$(P*4/nmmz* Hull and Berastegui, 2004), $CsCu_2I_3$(C*mcm* Hull and Berastegui, 2004), $CsAg_2I_3$(C*mcm* Hull and Berastegui, 2004), $CsCuI_3$(I*4/mmm*), $CsAgI_3$(I*4/mmm*). The decomposition pathways and enthalpies (ΔHd) is shown in Table S1.

Table S1 The decomposition pathways and enthalpies (ΔH_d)

1B-based PVSK	The decomposition pathways	The decomposition enthalpies (ΔH_d eV/atom)
$CsAuI_3$	$CsAuI_3 \rightarrow CsI+AuI+1/2I_2$	0.444
	$CsAuI_3 \rightarrow CsI+AuI_2$	0.447
	$CsAuI_3 \rightarrow CsI+AuI_3-1/2I_2$	0.339
Cs_2AgAuI_6	$Cs_2AgAuI_6 \rightarrow 2CsI+AgI+AuI+I_2$	0.594
	$Cs_2AgAuI_6 \rightarrow 2CsI+AgI+AuI_2+1/2I_2$	0.596
	$Cs_2AgAuI_6 \rightarrow 2CsI+AgI+AuI_3$	0.488
	$Cs_2AgAuI_6 \rightarrow CsI+AgI+CsAuI_3+1/2I_2$	0.150
	$Cs_2AgAuI_6 \rightarrow 2CsI+AgI_2+AuI+1/2I_2$	0.906
	$Cs_2AgAuI_6 \rightarrow 2CsI+AgI_2+AuI_2$	0.908
	$Cs_2AgAuI_6 \rightarrow 2CsI+AgI_2+AuI_3-1/2I_2$	0.800
	$Cs_2AgAuI_6 \rightarrow CsI+AgI_2+CsAuI_3$	0.462
	$Cs_2AgAuI_6 \rightarrow 2CsI+1/2Ag_2I_3+AuI+3/4I_2$	0.844
	$Cs_2AgAuI_6 \rightarrow 2CsI+1/2Ag_2I_3+AuI_2+1/4I_2$	0.846
	$Cs_2AgAuI_6 \rightarrow 2CsI+1/2Ag_2I_3+AuI_3-1/4I_2$	0.738
	$Cs_2AgAuI_6 \rightarrow CsI+1/2Ag_2I_3+CsAuI_3+1/4I_2$	0.400
	$Cs_2AgAuI_6 \rightarrow CsI+CsAgI_2+AuI+I_2$	0.582
	$Cs_2AgAuI_6 \rightarrow CsI+CsAgI_2+AuI_2+1/2I_2$	0.585
	$Cs_2AgAuI_6 \rightarrow CsI+CsAgI_2+AuI_3$	0.477
	$Cs_2AgAuI_6 \rightarrow CsAgI_2+CsAuI_3+1/2I_2$	0.138
	$Cs_2AgAuI_6 \rightarrow 3/2CsI+1/2CsAg_2I_3+AuI+I_2$	0.570
	$Cs_2AgAuI_6 \rightarrow 3/2CsI+1/2CsAg_2I_3+AuI_2+1/2I_2$	0.573
	$Cs_2AgAuI_6 \rightarrow 3/2CsI+1/2CsAg_2I_3+AuI_3$	0.465
	$Cs2AgAuI6 \rightarrow 1/2CsI+1/2CsAg_2I_3+CsAuI_3+1/2I_2$	0.126
	$Cs_2AgAuI_6 \rightarrow CsI+CsAgI_3+AuI+1/2I_2$	0.554
	$Cs_2AgAuI_6 \rightarrow CsI+CsAgI_3+AuI_2$	0.557
	$Cs_2AgAuI_6 \rightarrow CsI+CsAgI_3+AuI_3-1/2I_2$	0.449
	$Cs_2AgAuI_6 \rightarrow CsAgI_3+CsAuI_3$	0.110
Cs_2CuAuI_6	$Cs_2CuAuI_6 \rightarrow 2CsI+CuI+AuI+I_2$	0.646
	$Cs_2CuAuI_6 \rightarrow 2CsI+CuI+AuI_2+1/2I_2$	0.649

	$Cs_2CuAuI_6 \rightarrow 2CsI+CuI+AuI_3$	0.541
	$Cs_2CuAuI_6 \rightarrow CsI+CuI+CsAuI_3+1/2I_2$	0.202
	$Cs_2CuAuI_6 \rightarrow 2CsI+CuI_2+AuI+1/2I_2$	0.806
	$Cs_2CuAuI_6 \rightarrow 2CsI+CuI_2+AuI_2$	0.809
	$Cs_2CuAuI_6 \rightarrow 2CsI+CuI_2+AuI_3-1/2I_2$	0.701
	$Cs_2CuAuI_6 \rightarrow CsI+CuI_2+CsAuI_3$	0.362
	$Cs_2CuAuI_6 \rightarrow 2CsI+1/2Cu_2I_3+AuI+3/4I_2$	0.933
	$Cs_2CuAuI_6 \rightarrow 2CsI+1/2Cu_2I_3+AuI_2+1/4I_2$	0.935
	$Cs_2CuAuI_6 \rightarrow 2CsI+1/2Cu_2I_3+AuI_3-1/4I_2$	0.827
	$Cs_2CuAuI_6 \rightarrow CsI+1/2Cu_2I_3+CsAuI_3+1/4I_2$	0.489
	$Cs_2CuAuI_6 \rightarrow CsI+CsCuI_2+AuI+I_2$	0.880
	$Cs_2CuAuI_6 \rightarrow CsI+CsCuI_2+AuI_2+1/2I_2$	0.883
	$Cs_2CuAuI_6 \rightarrow CsI+CsCuI_2+AuI_3$	0.775
	$Cs_2CuAuI_6 \rightarrow CsCuI_2+CsAuI_3+1/2I_2$	0.436
	$Cs_2CuAuI_6 \rightarrow 3/2CsI+1/2CsCu_2I_3+AuI+I_2$	0.611
	$Cs_2CuAuI_6 \rightarrow 3/2CsI+1/2CsCu_2I_3+AuI_2+1/2I_2$	0.613
	$Cs_2CuAuI_6 \rightarrow 3/2CsI+1/2CsCu_2I_3+AuI_3$	0.505
	$Cs_2CuAuI_6 \rightarrow 1/2CsI+1/2CsCu_2I_3+CsAuI_3+1/2I_2$	0.167
	$Cs_2CuAuI_6 \rightarrow CsI+CsCuI_3+AuI+1/2I_2$	0.542
	$Cs_2CuAuI_6 \rightarrow CsI+CsCuI_3+AuI_2$	0.545
	$Cs_2CuAuI_6 \rightarrow CsI+CsCuI_3+AuI_3-1/2I_2$	0.437
	$Cs_2CuAuI_6 \rightarrow CsCuI_3+CsAuI_3$	0.098

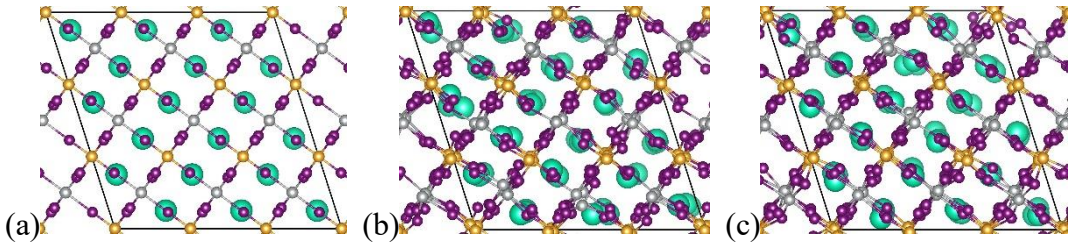

Figure S1 The structures during (a)0.0 ps, (b)0.5ps and (c)1.0ps AIMD simulations for Cs_2AgAuI_6 at 300K.

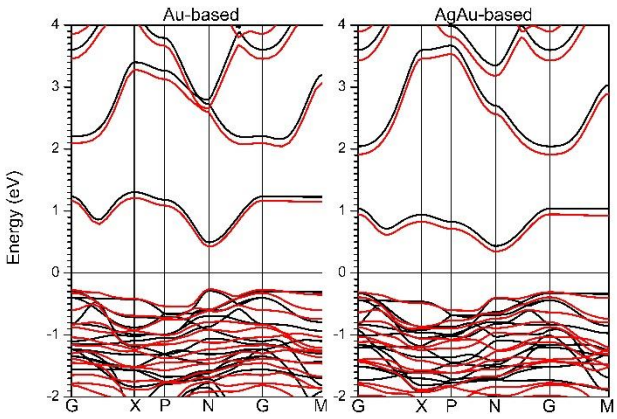

Figure S2 The PBE(black line) and PBE+SOC(red line) band structures of 1B-based perovskite solar cells absorbers.

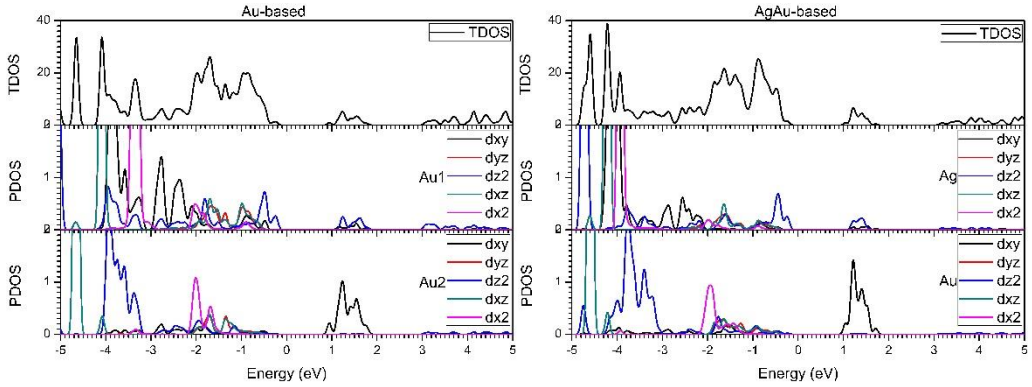

FigureS3 The HSE PDOS of 1B-based perovskite solar cells absorbers.

References

Ibberson R. M., Moze O., and Petrillo C. (1992). High resolution neutron powder diffraction studies of the low temperature crystal structure of molecular iodine (I_2). *Molecular Physics,* 76, 395-403. doi: 10.1080/00268979200101411

Keen D. A., and Hull S. (1995). The high-temperature structural behaviour of copper(I) iodide. *Journal of Physics: Condensed Matter* 7, 5793-5804. doi: 10.1088/0953-8984/7/29/007

Adipranoto D. S., Shikanai F., Yonemura M., Mori K., Park J. G., Itoh K., and Kamiyama T. (2009). Structure-property relationships of fast copper ion conductor cubic CuI. *Solid State Ionics* 180, 492-496. doi: 10.1016/j.ssi.2008.09.025

Jagodzinski, H. (1959). Die Kristallstruktur des AuJ. *Zeitschrift für Kristallographie* 112, 80-87. doi: 10.1524/zkri.1959.112.jg.80

Dell'amico D. B., Calderazzo F., Marchetti F., and Merlino S. (1982). Synthesis and molecular structure of Au_4Cl_8 and the isolation of $(Pt(CO)Cl_5)^-$ in thionyl chloride. *Journal of the Chemical Society. Dalton Transactions* 1982, 2257-2260. doi: 10.1039/DT9820002257

Clark E. S., Templeton D. H., and MacGillavry C. H. (1958). The crystal structure of gold(III) chloride. *Acta Crystallographica* 11, 284-288. doi: 10.1107/S0365110X58000694

Hull S., and Berastegui P. (2004). Crystal structures and ionic conductivities of ternary derivatives of the silver and copper monohalides-II: ordered phases within the $(AgX)_x$-$(MX)_{1-x}$ and $(CuX)_x$-$(MX)_{1-x}$ (M= K, Rb and Cs; X= Cl, Br and I) systems. *Journal of Solid State Chemistry* 177, 3156-3173. doi: 10.1016/j.jssc.2004.05.004